Author Manuscript

Author Manuscript

Author Manuscript

Author Manuscript

HHS Public Access

Author manuscript

Mol Genet Metab. Author manuscript; available in PMC 2018 March 01.

Published in final edited form as:

Mol Genet Metab. 2017 March ; 120(3): 288–294. doi:10.1016/j.ymgme.2016.12.006.

Combined alpha-delta platelet storage pool deficiency is associated with mutations in *GFI1B*

Carlos R. Ferreira[1,2], **Dong Chen**[3], **Shirley M. Abraham**[4], **David R. Adams**[1,5,6], **Karen L. Simon**[1], **May C. Malicdan**[1,5], **Thomas C. Markello**[5], **Meral Gunay-Aygun**[1,7], and **William A. Gahl**[1,5,6]

[1]Medical Genetics Branch, National Human Genome Research Institute, National Institutes of Health, Bethesda, MD

[2]Division of Genetics and Metabolism, Children's National Health System, Washington, DC

[3]Special Coagulation Laboratory, Division of Hematopathology, Department of Laboratory Medicine and Pathology, Mayo Clinic College of Medicine, Rochester, MN

[4]Division of Hematology and Oncology, Department of Pediatrics, University of New Mexico, Albuquerque, NM

[5]NIH Undiagnosed Diseases Program, NIH Common Fund, National Institutes of Health, Bethesda, MD

[6]Office of the Clinical Director, National Human Genome Research Institute, National Institutes of Health, Bethesda, MD

[7]Johns Hopkins University School of Medicine, Department of Pediatrics and McKusick-Nathans Institute of Genetic Medicine, Baltimore, MD

Abstract

Combined alpha-delta platelet storage pool deficiency is characterized by the absence or reduction in the number of both alpha granules and dense bodies. This disorder can have variable severity as well as a variable inheritance pattern. We describe two patients from unrelated families with combined alpha-delta storage pool deficiency due to mutations in *GFI1B*, a zinc finger protein known to act as a transcriptional repressor of various genes. We demonstrate that this disease is associated with either a heterozygous mutation (de novo or familial) abrogating the binding of the

Corresponding author: Carlos R. Ferreira, 10 Center Drive, MSC 1851, Building 10, Room 10C-103, Bethesda, Maryland 20892-1851, Phone: 301-402-7386, Fax: 301-480-9900, ferreiracr@mail.nih.gov.

Authorship

Contributions: CRF wrote the initial draft of the manuscript. DC provided expert platelet pathology interpretation. KLS and MCM performed genetic sequencing. DA and MGA provided management and clinical information for patient 1, while SMA provided clinical management for patient 2. TCM analyzed whole exome sequencing data in patient 1. WAG assisted with manuscript preparation and oversaw the study. All authors read and approved the final manuscript.

Disclosure of Conflicts of Interest

The authors declare that they have no competing financial interests.

Publisher's Disclaimer: This is a PDF file of an unedited manuscript that has been accepted for publication. As a service to our customers we are providing this early version of the manuscript. The manuscript will undergo copyediting, typesetting, and review of the resulting proof before it is published in its final citable form. Please note that during the production process errors may be discovered which could affect the content, and all legal disclaimers that apply to the journal pertain.

Author Manuscript Author Manuscript Author Manuscript Author Manuscript

zinc fingers with the promoter of its target genes, or by hypomorphic biallelic mutations in *GFI1B* leading to autosomal recessive inheritance.

Keywords

Combined alpha-delta platelet storage pool deficiency; αδ-SPD; *GFI1B*

1. Introduction

Normal platelets have 4–8 dense bodies and numerous alpha granules; combined alpha-delta platelet storage pool deficiency (αδ-SPD, OMIM 185050) is defined as the absence or severe deficiency of both alpha and delta granules. In 1979, Weiss et al. first described αδ-SPD in 7 patients [1], followed by a few reports of patients with quite heterogeneous presentations. Indeed, αδ-SPD can be inherited either in an autosomal dominant manner [1,2] or appear sporadically [1,3,4]. The severity of granule deficiency also varies [1], along with the surface expression of platelet markers [5]. Since the original description of αδ-SPD, its etiology has remained elusive, partly because of the scarcity of published reports, and partly because of the heterogeneity of the disease.

Isolated deficiency of dense granules characterizes Hermansky-Pudlak Syndrome (HPS), a disorder of lysosome-like organelles presenting with oculocutaneous albinism, a bleeding diathesis and, in 3 of the 10 genetic subtypes of HPS, pulmonary fibrosis. Isolated alpha granule deficiency is called Gray Platelet Syndrome (GPS), based upon the gray appearance of platelets on Wright stain. The genetic basis of GPS was elucidated by three different groups, who demonstrated that biallelic mutations in *NBEAL2* cause this disorder [6–8]. Recently, a monoallelic mutation in *GFI1B* was also reported to cause GPS, characterized by macrothrombocytopenia, reduced or absent alpha granules, and dysplastic megakaryocytes [9]. In addition, a *GFI1B* mutation segregated with an isolated bleeding diathesis of variable severity in a family with mild to moderate macrothrombocytopenia and subtle red cell changes consisting of anisopoikylocytosis and increased red blood cell distribution width [10,11], and in a family with thrombocytopenia, enlarged hypogranular platelets and abnormally shaped red blood cells [12]. Indeed, GFI1B is known to participate in both megakaryopoiesis and erythropoiesis [13,14].

We now demonstrate that both autosomal dominant and autosomal recessive αδ-SPD are associated with mutations in *GFI1B*.

2. Methods

2.1. Patients

Patients were enrolled in clinical protocol 76-HG-0238, “Diagnosis and treatment of patients with inborn errors of metabolism and other genetic disorders” (identifier: NCT00369421), approved by the NHGRI Institutional Review Board. Parents gave written, informed consent for their children, in accordance with the Declaration of Helsinki.

Author Manuscript Author Manuscript Author Manuscript Author Manuscript

2.2. Electron microscopy

Whole mount and thin section electron microscopy was performed as previously described [15,16]. Briefly, blood was collected into an ACD tube at room temperature, and the sample was centrifuged to obtain platelet rich plasma (PRP). For the whole mount technique, small drops of the PRP were placed on formvar-coated electron microscopy grids, rinsed for 10–15 s with drops of distilled water, dried from the periphery with filter paper and waved in the air to remove any residual moisture. The grids were then inserted into the electron microscope unfixed and unstained. Whole mount electron microscopy of a typical normal platelet is shown in Fig. 1A. The dense granules are dark opaque round-shaped bodies. Both dense granule calling criteria and the normal range of mean dense granules/platelet is ≥ 1.2 based on a normal donor study of 111 healthy volunteers were previously reported [17].

For thin sections, the samples were mixed with an equal volume of 0.1% glutaraldehyde buffered in White's saline. The samples were then centrifuged and the supernatant removed and replaced with 3% glutaraldehyde in White saline. This sample was then maintained at 4°C for 30 min and sedimented to pellet. The supernant was removed and replaced with 1% osmic acid. The samples were then dehydrated with alcohol, embedded in resin, and cut in thin sections using an ultramicrotome. Thin section electron microscopy of a normal platelet is shown in Fig. 1B.

Light microscopy images were obtained using an Olympus BX51 microscope (Olympus Life Science, Center Valley, PA) equipped with an Olympus DP71 camera; image at 1000x obtained using a UplanSApo 100x oil immersion objective lens and a UIS2 10x lens (Olympus). Electron microscopy images were obtained using a JEOL-1400Plus 120 kV transmission electron microscope (JEOL Ltd, Tokyo, Japan), with an Orius model 832 camera and DigitalMicrograph® acquisition software (Gatan Inc, Pleasanton, CA); pictures taken at 15,000–20,000X.

2.3. Sequencing

DNA was extracted from leucocytes using standard methods. Exome sequencing was performed in patient 1 as previously described [18]. Briefly, data were generated using an Illumina TruSeq Exome capture kit and the HiSeq2000 sequencing platform (Illumina, Inc, San Diego, CA). Reads were aligned with human reference genome hg19 (NCBI build 37; Feb. 2009) using Novoalign (Novocraft Technologies, Selangor, Malaysia). Variant calling was performed using the Most Probable Genotype (MPG) algorithm [19]. Called variants were annotated using a custom built process, then analyzed using VarSifter [20]. Initial sequence variant analysis was performed using an autosomal recessive genetic model. A second round of analysis employed a new-dominant model, identifying sequence variants that met the following criteria: (1) excellent coverage in all samples from prior Undiagnosed Diseases Program [21] next-generation sequencing projects; (2) variation from the human reference sequence occurring in only the family being studied; and (3) appearance of the candidate mutation only in affected members of the family.

Sanger sequencing was performed in patient 2. All exon and intron-exon boundaries of *GFI1B* were amplified by polymerase chain reaction (PCR) using genomic DNA as

Author Manuscript Author Manuscript Author Manuscript Author Manuscript

template. PCR was performed in a final volume of 10 μl containing 50 ng of genomic DNA, 1 μM of forward and reverse primers, and 5 μl of AmpliTaq Gold Master Mix (Applied Biosystems, Waltham, MA). The PCR products were purified using ExoSap-IT for 45 min at 37°C and sequenced in both directions using the same primers and Big Dye terminator kit v3.1 (Applied Biosystems). Reactions were purified over G-50 Sephadex. Linear amplification products were separated in an automated capillary sequencer (ABI PRISM 3130xl Genetic Analyzer, Applied Biosystems). Sequences were analyzed with Sequencher software 4.8 (Gene Codes Corporation, Ann Arbor, MI). Primer sequences are shown in supplementary file 1.

3. Results

3.1. Cases

Patient 1 is a 13-year-old boy born full term to non-consanguineous parents. Scalp petechiae were noted immediately after birth; evaluation revealed severe thrombocytopenia (platelets as low as 3,000/μL), as well as anemia and a granulocytic left shift. A head CT showed enlargement of the cysterna magna and right lateral ventricle. The infant received platelet transfusions at birth with a less than expected recovery of his platelet count. No platelet antibodies were detected. His anemia and left shift corrected spontaneously over the first few months of life, while the thrombocytopenia persisted. Other pertinent findings included subglandular hypospadias and chordee needing urethroplasty, bilateral partial 2–3 toe syndactyly (also present in his sister and maternal aunt), a Factor V Leiden mutation (c. 1691G>A, p.Arg506Gln) inherited from his mother, and right-sided periventricular nodular heterotopia with ipsilateral ventriculomegaly. He developed seizures at 5 years of age.

Over the course of his lifetime, patient 1 had easy bruising and petechiae, mainly in the face, neck folds, and extremities, as well as episodes of prolonged epistaxis and bleeding with injuries that did not respond promptly to DDAVP. Platelet counts averaged from 30–40,000/uL, but platelet transfusions were required several times for platelet counts under 10,000/uL. A trend of his pertinent blood counts over the first two years of life is provided in supplementary file 2.

A platelet function assay at 8 months showed a collagen/epinephrine membrane closure time of > 300 s (reference: 80–144) and a collagen/ADP closure time of > 250 s (ref: 45–110). A bone marrow aspirate and biopsy at 2 months showed a hypercellular marrow (98%) with scattered megakaryocytes that were decreased in number, confirmed through immunostaining for von Willebrand factor. The platelets were variable in size; some were quite small, with decreased cytoplasm. Red cell maturation appeared progressive, but the cytoplasm of late normoblasts appeared somewhat ragged. Myeloid maturation was also progressive, but a left shift was appreciated with a relative decrease in mature segmented neutrophils. A repeat bone marrow aspirate and biopsy at 11 months showed a decreased number of small megakaryocytes with one or two large irregular nuclei and abnormally scant cytoplasm showing rare platelet formation. Granulocytic maturation was abnormal, showing hypogranulation. A concurrent peripheral smear showed a circulating megakaryocyte with single abnormal convoluted nucleus and cytoplasm showing numerous small blebs. Platelet electron microscopy at 3 months revealed a total of 21 dense granules

Author Manuscript Author Manuscript Author Manuscript Author Manuscript

within 100 whole mounted platelets–with 83% of platelets having no dense granules and 17% having 1–2 dense granules per platelet–consistent with a severe delta granule storage pool deficiency (figures 1C–1D). Thin sections of the buffy coat using transmission electron microscopy demonstrated platelets (about 2–5 micrometers in diameter) with an additional alpha granule deficiency (figures 1E–1F). Other than granular deficiency, some morphologic abnormalities such as enlarged mitochondria (figure 1E) and empty vacuoles (figure 1H) were seen. Other platelet components such as the circumferential microtubules (figure 1G) and the dense tubular system (figure 1I) were unremarkable. Most of the granulocytes present in the buffy coat were also unusual in their morphology and appeared to be in blastic phase or undergoing apoptosis.

Patient 2 is an 8-year-old male born to Mexican parents who denied consanguinity. At 3 months of age he had multiple spontaneous petechiae along with isolated thrombocytopenia (platelet count 46,000/μL). At 10 months, a bone marrow biopsy showed increased megakaryocytes suggestive of idiopathic thrombocytopenic purpura. By 3 years of age, he had received three treatments with intravenous immunoglobulins (IVIG) without adequate response. Platelet counts ranged from 30,000 to 50,000/μL at baseline, dropping to 15,000 to 20,000 with acute illnesses. The primary bleeding symptoms included spontaneous bruising, petechiae, and prolonged epistaxis, generally well controlled with anti-fibrinolytic agents, although platelet transfusions were required for significant bleeds and surgical procedures.

Over the past 5 years, peripheral smears showed atypical large platelets and hypogranular platelets (figure 1J), and two additional bone marrow aspirates showed megakaryocytic hyperplasia with numerous osteoclast-like forms, occasional small monolobated megakaryocytes, and emperipolesis (figure 1K). On whole mount electron microscopy, the platelets contained virtually no dense granules (0.05 dense granules per platelet, 200 platelets counted; figure 1L). On thin section electron microscopy, 30–40% of platelets (about 2–5 micrometers in diameter) had markedly decreased numbers of alpha granules (figures 1N–1O).

3.2. Genetics

Family pedigrees for patients 1 and 2 are shown in figures 2A and 2B, respectively. For patient 1, prior genetic testing included normal *TPO* and *GATA1* sequencing and a normal chromosome microarray. At the NIH, we performed whole exome sequencing and found a heterozygous nonsense mutation in *GFI1B*, i.e., NM_004188.5:c.793A>T (NP_004179.3:p.Lys265*; figure 2C). The mutation appeared *de novo*, as it was not seen in either parent, and paternity was confirmed based on the inheritance of polymorphisms using next generation sequencing data. Depth of coverage was 124x at that position, with 60 reads showing the reference allele and 64 reads showing the minor allele; of the latter, 26 reads were from the plus strand and 38 reads belonged to the minus strand, ruling out strand bias. The mutation was confirmed by Sanger sequencing (supplementary file 3). This truncating mutation is exceedingly rare, as it was not found in 60,706 individuals in the Exome Aggregation Consortium (ExAC, Cambridge, MA) [22]. The amino acid at that position is well conserved through evolution (supplementary file 4) [23], and the mutation has a high Phred-scaled CADD score of 43, consistent with a nonsense mutation [24]. Despite the fact

Author Manuscript Author Manuscript Author Manuscript Author Manuscript

that this mutation is truncating, the transcript is predicted to escape nonsense-mediated decay, because the mutation is located only 22 nucleotides upstream of the last exon-exon junction [25].

Given the finding of a *GFI1B* mutation in patient 1 with αδ-SPD, Sanger sequencing was performed directly on the *GFI1B* gene of patient 2. A homozygous mutation was found: NM_004188.5:c.923T>C (NP_004179.3:p.Leu308Pro; figure 2D). Each parent had one copy of this mutation (figure 2D). The change occurred in a highly conserved amino acid position (supplementary file 5) [23], and is present in only 1 of 121,194 alleles in the general population and, in particular, in 1 of 11,570 alleles in the Latino population [22]. In silico algorithms predict it to be pathogenic; Polyphen-2 predicts it to be probably damaging [26], SIFT predicts the change to be deleterious [27], and CADD assigns it a Phred-scaled score of 27.5 [24].

Both mutations in our patients are located within C-terminal zinc finger regions. The mutation of patient 1 is located in zinc finger 4 (figure 2E), one of the three GFI1B zinc fingers (along with zinc fingers 3 and 5) responsible for DNA binding [28]. The truncated protein lacks amino acid residues responsible for hydrogen, electrostatic and hydrophobic bonds with DNA in zinc fingers 4 and 5 (figure 2F). The mutation on patient 2 is located in zinc finger 6 (figure 2E).

4. Discussion

Megakaryocytes and erythrocytes derive from the same bipotential progenitor cell, whose proliferation and differentiation are regulated by GFI1B [29]. During megakaryocytic differentiation, the megakaryoblast's DNA replicates without subsequent cell division in a process known as endomitosis, leading to a polyploid cell with multilobulated nuclei known as the promegakaryocyte. The cytoplasm of this cell subsequently expands to give rise to platelets. The conditional absence of *Gfi1b* in mice leads to arrest at the promegakaryocyte stage, after endomitosis is completed but before the maturation of the cytoplasm [30]. In erythrocytes, the conditional inactivation of *Gfi1b* leads to impaired differentiation of pro-erythroblasts to mature erythrocytes [31]. A long isoform of GFI1B that contains exon 5 is essential for megakaryopoiesis, while a short isoform lacking exon 5 is essential for its erythropoietic role [14].

GFI1B functions as a transcriptional repressor. Its C-terminal zinc fingers bind to DNA, specifically to the promoter region of target genes. The N-terminal SNAG domain recruits the protein machinery that represses transcription; these proteins include the corepressor CoREST, the histone demethylase LSD1, and the histone deacetylases HDAC1 and HDAC2 [32].

Heterozygous truncating mutations in *GFI1B* have previously been described in three families with autosomal dominant inheritance of macrothrombocytopenia and reduced alpha granules, as well as anisocytosis and poikilocytosis of red blood cells [33,10,11,9]. A comparison of findings in the three previously reported families, as well as in the present cases, is provided in Table 1. In the single family reported by Monteferrario et al., there was

Author Manuscript Author Manuscript Author Manuscript Author Manuscript

no mention of the number of delta granules, and in fact the thin section electron microscopy images shown reveal reduced or absent delta granules compared with the control image [9]. In the family reported by Stevenson et al. it is noted that dense granules appeared normal in all family members [11]. However, the same family was previously reported by Ardlie et al. in 1976, where it was mentioned that “there seemed to be paucity of dense bodies” on thin sections [10]. More importantly, there is no mention of whole mount electron microscopy being performed in either family; since dense bodies are inherently electron opaque, it is more accurate to evaluate their number by whole mount electron microscopy than by thin sections [2]. Finally, murine megakaryocytes conditionally deficient in *Gfi1b* have substantially reduced numbers of dense bodies [34].

In all previously reported families, a truncating mutation (nonsense in Monteferrario et al. [9], frameshift in Stevenson et al. [11] and canonical splice site in Kitamura et al. [12]) was identified in or proximal to the fifth zinc finger domain, while in patient 1 in this report a truncating nonsense mutation was identified in the fourth zinc finger domain. The three previously reported truncating mutations have been shown to escape nonsense-mediated decay and to exert a dominant negative effect, inhibiting the transcriptional repression activity of the protein [9,11,12]. It is predicted that, as in the case of the three previously described mutations, the truncating variant found in patient 1 will also escape nonsense-mediated decay, since it is located fewer than 50–55 nucleotides upstream of the last exon-exon junction [25]. The autosomal dominant pattern of inheritance can be explained by a dominant negative mechanism through loss of amino acids participating in DNA binding (figure 1F), since the expressed truncated protein will interfere with the wild-type protein by competing for the same DNA binding sites, or by quenching the effects of other cofactors of the transcriptional machinery. Haploinsufficiency of *Gfi1b* in a mouse model leads to no demonstrable abnormalities, while a homozygous deletion leads to fetal lethality [13]. Thus, completely absent GFI1B repressional activity is not compatible with life, and 50% residual activity is not associated with any clinical consequences. The autosomal recessive pattern of inheritance seen in patient 2 is thus likely explained by hypomorphic loss-of-function mutations. It is unknown how missense variants alter protein function. An altered tertiary structure could either decrease the DNA-binding capacity, or occupy DNA binding sites while lacking the capacity to bind cofactors. Thus, uncertainty remains concerning the precise mechanism leading to the reported phenotype, and whether the severity could be modulated by variants in other, modifying genes.

As can be seen in table 1, a common finding in bone marrow biopsy seems to be that of dysplastic megakaryocytes and emperipolesis. It is more difficult, however, to generalize regarding the number of megakaryocytes, as they have been variously described as decreased (patient 1), normal to slightly increased [33], or increased in number (patient 2 and [9]). It is likely that these differences stem from the fact that the number of megakaryocytes in the bone marrow has been assessed subjectively.

Patient 1 showed a left shift and a relative decrease in the number of mature bone marrow granulocytes early in life. GFI1B is not expressed in granulocyte-monocyte progenitor cells; however, it is then re-expressed in circulating monocytes and granulocytes, pointing towards a role in mobilizing these cells from the bone marrow to the periphery [35]. In fact,

Author Manuscript Author Manuscript Author Manuscript Author Manuscript

immature myeloid cells and monocytes, as well as a reduced number of granulocytes, have previously been described in the bone marrow of Gfi1$^{1b/1b}$ knock-in mice [36]. The reason for the spontaneous resolution of anemia seen in patient 1–and the lack of a more prominent red blood cell phenotype in general in patients with GFI1B deficiency–is puzzling, especially considering that GFI1B is still needed for adult erythropoiesis, just as it is for adult megakaryopoiesis [30].

Mutations in another transcription factor, *GATA1*, lead to dyserythropoietic anemia, macrothrombocytopenia, and deficiency of alpha granules [37]. In addition, some mutations in this X-linked gene cause absence of both alpha and delta granules [38]. The similar phenotypes caused by mutations in these two transcription factors is not surprising, especially in light of the fact that GFI1B is known to interact with GATA1 [39–41].

Both patients described here had congenital anomalies, including hypospadias, periventricular nodular heterotopia and syndactyly in patient 1, and persistent patent ductus arteriosus in patient 2. The syndactyly in patient 1 is likely unrelated to the *GFI1B* mutation, as it segregated independently in the family. It is unknown, however, if the other anomalies are related to the *GFI1B* variants, or to variants in other genes. Even assuming that variants in other genes were to be found, these would be unlikely to explain the paucity of delta granules, since the fact that the two unrelated patients described here both had decreased number of delta granules and rare variants in *GFI1B* likely means that there is an association between these findings. In addition, as previously explained, experimental animal data support the role of *GFI1B* deficiency in dense body reduction [34].

In conclusion, we demonstrate that αδ-SPD is associated with mutations in *GFI1B*. Our finding of the underlying etiology of αδ-SPD not only expands the known spectrum of pathology associated with mutations in *GFI1B*, but should open new avenues of investigation into novel therapeutic options for this rare disorder. As an example, it is known that valproic acid, a histone deacetylase inhibitor, induces expression of GFI1B [42]. Further investigations carry the potential to develop interventions that could change the course of αδ-SPD and related disorders.

Supplementary Material

Refer to Web version on PubMed Central for supplementary material.

Acknowledgments

This study was supported by the Intramural Research Program of the National Human Genome Research Institute, National Institutes of Health. The authors thank the patients and their families for their kind support and assistance. We dedicate this work to the late Dr. James G. White, who contributed to the evaluation of patient 1.

References

1. Weiss HJ, Witte LD, Kaplan KL, Lages BA, Chernoff A, Nossel HL, Goodman DS, Baumgartner HR. Heterogeneity in storage pool deficiency: studies on granule-bound substances in 18 patients including variants deficient in alpha-granules, platelet factor 4, beta-thromboglobulin, and platelet-derived growth factor. Blood. 1979; 54:1296–1319. [PubMed: 508939]

Author Manuscript Author Manuscript Author Manuscript Author Manuscript

2. White JG, Keel S, Reyes M, Burris SM. Alpha-delta platelet storage pool deficiency in three generations. Platelets. 2007; 18:1–10. DOI: 10.1080/09537100600800172

3. Kosch A, Kehrel B, Nowak-Göttl U, Häberle J, Jürgens H. Thrombocytic alpha-delta-storage-pool-disease: shortening of bleeding time after infusion of 1-desamino-8-D-arginine vasopressin. Klin Pädiatr. 1999; 211:198–200. DOI: 10.1055/s-2008-1043787 [PubMed: 10472549]

4. Biddle DA, Neto TG, Nguyen AN. Platelet storage pool deficiency of alpha and delta granules. Arch Pathol Lab Med. 2001; 125:1125–1126. DOI: 10.1043/0003-9985(2001)125<1125:PSPDOA>2.0.CO;2 [PubMed: 11473478]

5. Lages B, Shattil SJ, Bainton DF, Weiss HJ. Decreased content and surface expression of alpha-granule membrane protein GMP-140 in one of two types of platelet alpha delta storage pool deficiency. J Clin Invest. 1991; 87:919–929. DOI: 10.1172/JCI115099 [PubMed: 1705568]

6. Gunay-Aygun M, Falik-Zaccai TC, Vilboux T, Zivony-Elboum Y, Gumruk F, Cetin M, Khayat M, Boerkoel CF, Kfir N, Huang Y, Maynard D, Dorward H, Berger K, Kleta R, Anikster Y, Arat M, Freiberg AS, Kehrel BE, Jurk K, Cruz P, Mullikin JC, White JG, Huizing M, Gahl WA. NBEAL2 is mutated in gray platelet syndrome and is required for biogenesis of platelet α-granules. Nat Genet. 2011; 43:732–734. DOI: 10.1038/ng.883 [PubMed: 21765412]

7. Albers CA, Cvejic A, Favier R, Bouwmans EE, Alessi MC, Bertone P, Jordan G, Kettleborough RNW, Kiddle G, Kostadima M, Read RJ, Sipos B, Sivapalaratnam S, Smethurst PA, Stephens J, Voss K, Nurden A, Rendon A, Nurden P, Ouwehand WH. Exome sequencing identifies NBEAL2 as the causative gene for gray platelet syndrome. Nat Genet. 2011; 43:735–737. DOI: 10.1038/ng.885 [PubMed: 21765411]

8. Kahr WHA, Hinckley J, Li L, Schwertz H, Christensen H, Rowley JW, Pluthero FG, Urban D, Fabbro S, Nixon B, Gadzinski R, Storck M, Wang K, Ryu GY, Jobe SM, Schutte BC, Moseley J, Loughran NB, Parkinson J, Weyrich AS, Di Paola J. Mutations in NBEAL2, encoding a BEACH protein, cause gray platelet syndrome. Nat Genet. 2011; 43:738–740. DOI: 10.1038/ng.884 [PubMed: 21765413]

9. Monteferrario D, Bolar NA, Marneth AE, Hebeda KM, Bergevoet SM, Veenstra H, Laros-van Gorkom BAP, MacKenzie MA, Khandanpour C, Botezatu L, Fransen E, Van Camp G, Duijnhouwer AL, Salemink S, Willemsen B, Huls G, Preijers F, Van Heerde W, Jansen JH, Kempers MJE, Loeys BL, Van Laer L, Van der Reijden BA. A dominant-negative GFI1B mutation in the gray platelet syndrome. N Engl J Med. 2014; 370:245–253. DOI: 10.1056/NEJMoa1308130 [PubMed: 24325358]

10. Ardlie NG, Coupland WW, Schoefl GI. Hereditary thrombocytopathy: a familial bleeding disorder due to impaired platelet coagulant activity. Aust N Z J Med. 1976; 6:37–45.

11. Stevenson WS, Morel-Kopp MC, Chen Q, Liang HP, Bromhead CJ, Wright S, Turakulov R, Ng AP, Roberts AW, Bahlo M, Ward CM. GFI1B mutation causes a bleeding disorder with abnormal platelet function. J Thromb Haemost JTH. 2013; 11:2039–2047. DOI: 10.1111/jth.12368 [PubMed: 23927492]

12. Kitamura K, Okuno Y, Yoshida K, Sanada M, Shiraishi Y, Muramatsu H, Kobayashi R, Furukawa K, Miyano S, Kojima S, Ogawa S, Kunishima S. Functional characterization of a novel GFI1B mutation causing congenital macrothrombocytopenia. J Thromb Haemost JTH. 2016; 14:1462–1469. DOI: 10.1111/jth.13350 [PubMed: 27122003]

13. Saleque S, Cameron S, Orkin SH. The zinc-finger proto-oncogene Gfi-1b is essential for development of the erythroid and megakaryocytic lineages. Genes Dev. 2002; 16:301–306. DOI: 10.1101/gad.959102 [PubMed: 11825872]

14. Polfus LM, Khajuria RK, Schick UM, Pankratz N, Pazoki R, Brody JA, Chen MH, Auer PL, Floyd JS, Huang J, Lange L, van Rooij FJA, Gibbs RA, Metcalf G, Muzny D, Veeraraghavan N, Walter K, Chen L, Yanek L, Becker LC, Peloso GM, Wakabayashi A, Kals M, Metspalu A, Esko T, Fox K, Wallace R, Franceshini N, Matijevic N, Rice KM, Bartz TM, Lyytikäinen LP, Kähönen M, Lehtimäki T, Raitakari OT, Li-Gao R, Mook-Kanamori DO, Lettre G, van Duijn CM, Franco OH, Rich SS, Rivadeneira F, Hofman A, Uitterlinden AG, Wilson JG, Psaty BM, Soranzo N, Dehghan A, Boerwinkle E, Zhang X, Johnson AD, O'Donnell CJ, Johnsen JM, Reiner AP, Ganesh SK, Sankaran VG. Whole-Exome Sequencing Identifies Loci Associated with Blood Cell Traits and Reveals a Role for Alternative GFI1B Splice Variants in Human Hematopoiesis. Am J Hum Genet. 2016; 99:481–488. DOI: 10.1016/j.ajhg.2016.06.016 [PubMed: 27486782]

Author Manuscript Author Manuscript Author Manuscript Author Manuscript

15. White JG. Use of the electron microscope for diagnosis of platelet disorders. Semin Thromb Hemost. 1998; 24:163–168. DOI: 10.1055/s-2007-995836 [PubMed: 9579638]

16. White JG. Electron-dense chains and clusters in platelets from patients with storage pool-deficiency disorders. J Thromb Haemost JTH. 2003; 1:74–79. [PubMed: 12871542]

17. Uhl CB, Barness RL, Olson MC, Gossman SC, Erdogan S, Gamb SI, Charlesworth JE, Lingineni R, Bryant SC, Miller RS, Salisbury JL, Nichols WL, White JG. Platelet Storage Pool Deficiency: Establishment Of Reference Ranges For Platelet Dense Granule Count By Transmission Electron Microscopy. Blood. 2013; 122:3549.

18. Adams DR, Sincan M, Fuentes Fajardo K, Mullikin JC, Pierson TM, Toro C, Boerkoel CF, Tifft CJ, Gahl WA, Markello TC. Analysis of DNA sequence variants detected by high-throughput sequencing. Hum Mutat. 2012; 33:599–608. DOI: 10.1002/humu.22035 [PubMed: 22290882]

19. Teer JK, Bonnycastle LL, Chines PS, Hansen NF, Aoyama N, Swift AJ, Abaan HO, Albert TJ, Margulies EH, Green ED, Collins FS, Mullikin JC, Biesecker LG. NISC Comparative Sequencing Program. Systematic comparison of three genomic enrichment methods for massively parallel DNA sequencing. Genome Res. 2010; 20:1420–1431. DOI: 10.1101/gr.106716.110 [PubMed: 20810667]

20. Teer JK, Green ED, Mullikin JC, Biesecker LG. VarSifter: visualizing and analyzing exome-scale sequence variation data on a desktop computer. Bioinforma Oxf Engl. 2012; 28:599–600. DOI: 10.1093/bioinformatics/btr711

21. Gahl WA, Mulvihill JJ, Toro C, Markello TC, Wise AL, Ramoni RB, Adams DA, Tifft CJ. The NIH Undiagnosed Diseases Program and Network: Applications to modern medicine. Mol Genet Metab. 2016; 117:393–400. [PubMed: 26846157]

22. Lek M, Karczewski K, Minikel E, Samocha K, Banks E, Fennell T, O'Donnell-Luria A, Ware J, Hill A, Cummings B, Tukiainen T, Birnbaum D, Kosmicki J, Duncan L, Estrada K, Zhao F, Zou J, Pierce-Hoffman E, Cooper D, DePristo M, Do R, Flannick J, Fromer M, Gauthier L, Goldstein J, Gupta N, Howrigan D, Kiezun A, Kurki M, Levy Moonshine A, Natarajan P, Orozco L, Peloso G, Poplin R, Rivas M, Ruano-Rubio V, Ruderfer D, Shakir K, Stenson P, Stevens C, Thomas B, Tiao G, Tusie-Luna M, Weisburd B, Won H-H, Yu D, Altshuler D, Ardissino D, Boehnke M, Danesh J, Roberto E, Florez J, Gabriel S, Getz G, Hultman C, Kathiresan S, Laakso M, McCarroll S, McCarthy M, McGovern D, McPherson R, Neale B, Palotie A, Purcell S, Saleheen D, Scharf J, Sklar P, Patrick S, Tuomilehto J, Watkins H, Wilson J, Daly M, MacArthur D. Analysis of protein-coding genetic variation in 60,706 humans. 2015; bioRxiv. doi: 10.1101/030338

23. Kent WJ, Sugnet CW, Furey TS, Roskin KM, Pringle TH, Zahler AM, Haussler D. The human genome browser at UCSC. Genome Res. 2002; 12:996–1006. Article published online before print in May 2002. DOI: 10.1101/gr.229102 [PubMed: 12045153]

24. Kircher M, Witten DM, Jain P, O'Roak BJ, Cooper GM, Shendure J. A general framework for estimating the relative pathogenicity of human genetic variants. Nat Genet. 2014; 46:310–315. DOI: 10.1038/ng.2892 [PubMed: 24487276]

25. Nagy E, Maquat LE. A rule for termination-codon position within intron-containing genes: when nonsense affects RNA abundance. Trends Biochem Sci. 1998; 23:198–199. [PubMed: 9644970]

26. Adzhubei IA, Schmidt S, Peshkin L, Ramensky VE, Gerasimova A, Bork P, Kondrashov AS, Sunyaev SR. A method and server for predicting damaging missense mutations. Nat Methods. 2010; 7:248–249. DOI: 10.1038/nmeth0410-248 [PubMed: 20354512]

27. Kumar P, Henikoff S, Ng PC. Predicting the effects of coding non-synonymous variants on protein function using the SIFT algorithm. Nat Protoc. 2009; 4:1073–1081. DOI: 10.1038/nprot.2009.86 [PubMed: 19561590]

28. Lee S, Doddapaneni K, Hogue A, McGhee L, Meyers S, Wu Z. Solution structure of Gfi-1 zinc domain bound to consensus DNA. J Mol Biol. 2010; 397:1055–1066. DOI: 10.1016/j.jmb.2010.02.006 [PubMed: 20153336]

29. Randrianarison-Huetz V, Laurent B, Bardet V, Blobe GC, Huetz F, Duménil D. Gfi-1B controls human erythroid and megakaryocytic differentiation by regulating TGF-beta signaling at the bipotent erythro-megakaryocytic progenitor stage. Blood. 2010; 115:2784–2795. DOI: 10.1182/blood-2009-09-241752 [PubMed: 20124515]

30. Foudi A, Kramer DJ, Qin J, Ye D, Behlich A-S, Mordecai S, Preffer FI, Amzallag A, Ramaswamy S, Hochedlinger K, Orkin SH, Hock H. Distinct, strict requirements for Gfi-1b in adult bone

Author Manuscript Author Manuscript Author Manuscript Author Manuscript

marrow red cell and platelet generation. J Exp Med. 2014; 211:909–927. DOI: 10.1084/jem.20131065 [PubMed: 24711581]

31. Vassen L, Beauchemin H, Lemsaddek W, Krongold J, Trudel M, Möröy T. Growth factor independence 1b (gfi1b) is important for the maturation of erythroid cells and the regulation of embryonic globin expression. PloS One. 2014; 9:e96636.doi: 10.1371/journal.pone.0096636 [PubMed: 24800817]
32. Saleque S, Kim J, Rooke HM, Orkin SH. Epigenetic regulation of hematopoietic differentiation by Gfi-1 and Gfi-1b is mediated by the cofactors CoREST and LSD1. Mol Cell. 2007; 27:562–572. DOI: 10.1016/j.molcel.2007.06.039 [PubMed: 17707228]
33. Kurstjens R, Bolt C, Vossen M, Haanen C. Familial thrombopathic thrombocytopenia. Br J Haematol. 1968; 15:305–317. [PubMed: 5681484]
34. Vassen L, Moroy T. Growth Factor Independence 1b (Gfi1b) Is An Essential Regulator of Late Stage Megakaryocyte Maturation and Platelet Production. Blood. 2011; 118:2358. [PubMed: 21715305]
35. Vassen L, Okayama T, Möröy T. Gfi1b:green fluorescent protein knock-in mice reveal a dynamic expression pattern of Gfi1b during hematopoiesis that is largely complementary to Gfi1. Blood. 2007; 109:2356–2364. DOI: 10.1182/blood-2006-06-030031 [PubMed: 17095621]
36. Fiolka K, Hertzano R, Vassen L, Zeng H, Hermesh O, Avraham KB, Dührsen U, Möröy T. Gfi1 and Gfi1b act equivalently in haematopoiesis, but have distinct, non-overlapping functions in inner ear development. EMBO Rep. 2006; 7:326–333. DOI: 10.1038/sj.embor.7400618 [PubMed: 16397623]
37. White JG, Nichols WL, Steensma DP. Platelet pathology in sex-linked GATA-1 dyserythropoietic macrothrombocytopenia I ultrastructure. Platelets. 2007; 18:273–283. DOI: 10.1080/09537100601065825 [PubMed: 17538848]
38. White JG, Thomas A. Platelet structural pathology in a patient with the X-linked GATA-1, R216Q mutation. Platelets. 2009; 20:41–49. DOI: 10.1080/09537100802406661 [PubMed: 19172521]
39. Huang DY, Kuo YY, Lai JS, Suzuki Y, Sugano S, Chang ZF. GATA-1 and NF-Y cooperate to mediate erythroid-specific transcription of Gfi-1B gene. Nucleic Acids Res. 2004; 32:3935–3946. DOI: 10.1093/nar/gkh719 [PubMed: 15280509]
40. Rodriguez P, Bonte E, Krijgsveld J, Kolodziej KE, Guyot B, Heck AJR, Vyas P, de Boer E, Grosveld F, Strouboulis J. GATA-1 forms distinct activating and repressive complexes in erythroid cells. EMBO J. 2005; 24:2354–2366. DOI: 10.1038/sj.emboj.7600702 [PubMed: 15920471]
41. Anguita E, Villegas A, Iborra F, Hernández A. GFI1B controls its own expression binding to multiple sites. Haematologica. 2010; 95:36–46. DOI: 10.3324/haematol.2009.012351 [PubMed: 19773260]
42. Zini R, Norfo R, Ferrari F, Bianchi E, Salati S, Pennucci V, Sacchi G, Carboni C, Ceccherelli GB, Tagliafico E, Ferrari S, Manfredini R. AGIMM Investigators. Valproic acid triggers erythro/megakaryocyte lineage decision through induction of GFI1B and MLLT3 expression. Exp Hematol. 2012; 40:1043–1054.e6. DOI: 10.1016/j.exphem.2012.08.003 [PubMed: 22885124]
43. Bennett RL, French KS, Resta RG, Doyle DL. Standardized human pedigree nomenclature: update and assessment of the recommendations of the National Society of Genetic Counselors. J Genet Couns. 2008; 17:424–433. DOI: 10.1007/s10897-008-9169-9 [PubMed: 18792771]

Author Manuscript Author Manuscript Author Manuscript Author Manuscript

Highlights

- Combined alpha-delta storage pool deficiency is associated with monoallelic, dominant negative mutations or biallelic hypomorphic mutations in *GFI1B*.

Author Manuscript Author Manuscript Author Manuscript Author Manuscript

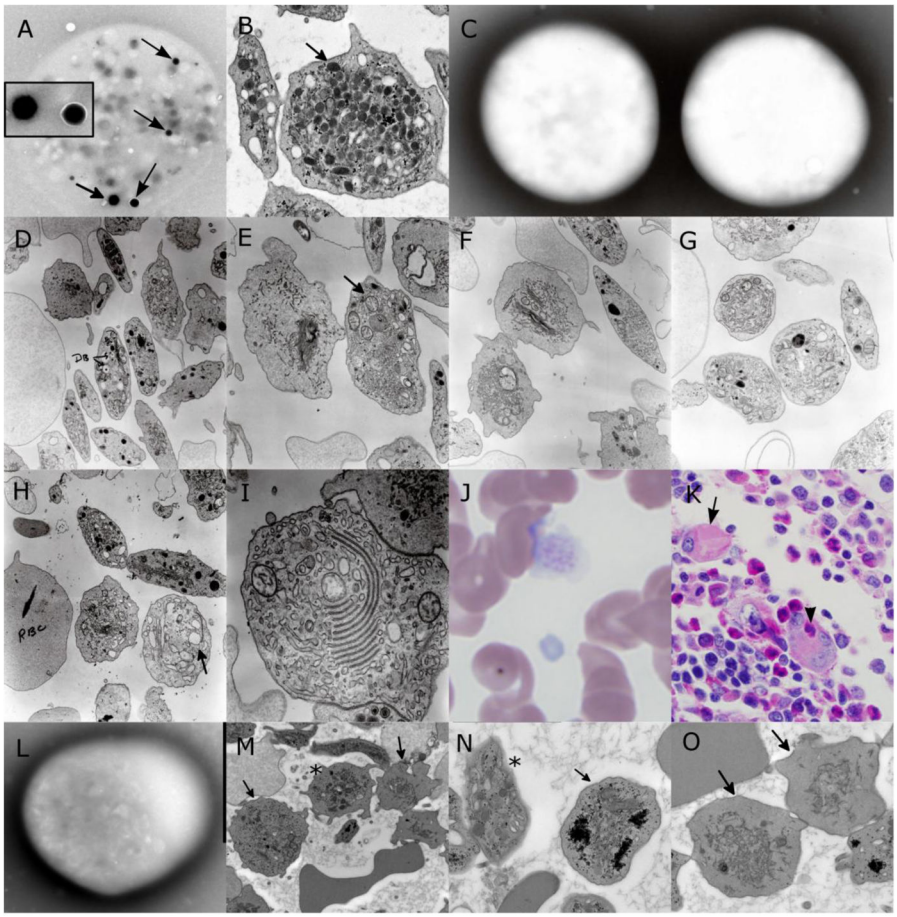

Figure 1. Light and electron microscopy of patients platelets and megakaryocytes

A: Whole mount electron microscopy of a platelet from a normal control donor. Arrow points to a dense granule. B: Thin section electron microscopy of platelet from a normal donor. Arrow points to an alpha granule. C: Dense bodies were virtually absent on whole mount electron microscopy of platelets from patient 1. D: Small dense bodies (DB) could be found in occasional platelets from patient 1 by thin section electron microscopy. E: Absent alpha granules inside platelets from patient 1; mitochondria have become the predominant organelle, and many are enlarged (arrow). F: Severely deficient–but present–alpha granules in platelets of patient 1. G: Platelets of patient 1 maintain a normal discoid shape, given the normal circumferential coils of microtubules in the equatorial plane. H: Marked increase in the number of granule-sized empty vacuoles (arrow) of some platelets from patient 1. I: Normal transition from rough endoplasmic reticulum to the dense tubular system elements in platelets from patient 1. J: Peripheral smear (Wright-Giemsa stain, 1000x) of patient 2 shows a large platelet with cytoplasmic granules and a smaller platelet without any granules. K: The megakaryocytes in the bone marrow biopsy from patient 2 show marked emperipolesis (arrow head) and apparent cytoplasmic pale pink inclusions (arrow, PAS stain, 400X). L: Whole mount electron microscopy of a platelet from patient 2 shows no dense granules. M: Thin section electron microscopy shows a platelet of patient 2 with alpha granules (*) and 2 other platelets (arrows) with rare (left) or no (right) alpha granules. N: A platelet of patient 2 with alpha granules (*) and a platelet with rare alpha granules (arrow).

Author Manuscript Author Manuscript Author Manuscript Author Manuscript

O: A high magnification image of two platelets (arrows) of patient 2 without (on the right) and with rare alpha granules (on the left).

Author Manuscript Author Manuscript Author Manuscript Author Manuscript

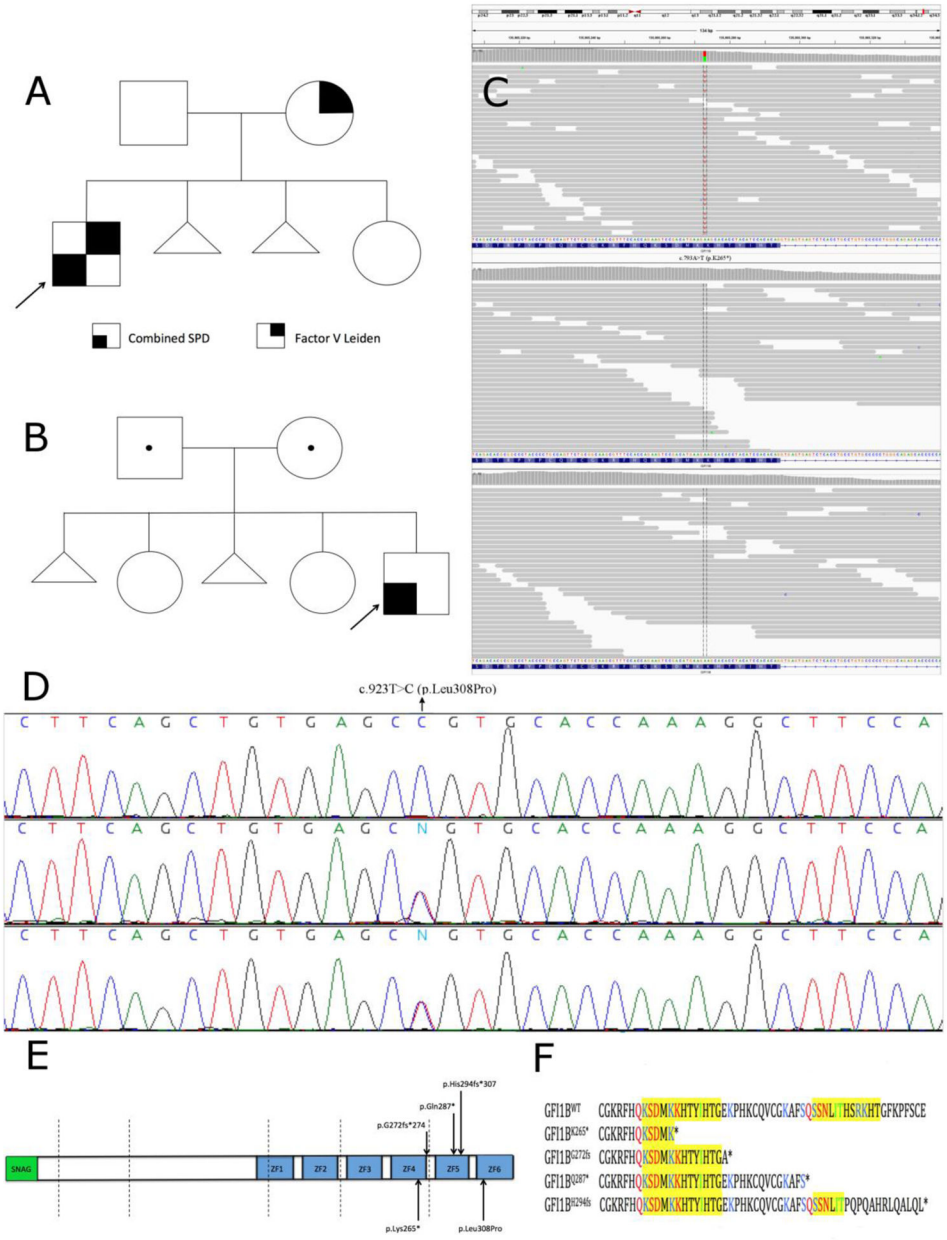

Figure 2. Genetics of αδ-SPD patients

A: Pedigree for patient 1. Squares denote male individuals and circles female individuals, while triangles represent spontaneous abortions, solid symbols affected family members, open symbols unaffected family members, and arrows indicate proband. Dotted symbols indicate carrier state. All symbols used in accordance with the standardized human pedigree nomenclature [43]. B: Pedigree for patient 2. C: Whole exome short read alignments to the reference sequence for patient 1 (top), his father (middle) and his mother (bottom). Patient 1 has a heterozygous change (A>T) in position 793 arising *de novo.* D: Sanger sequencing chromatograms for patient 2 (top), his father (middle) and his mother (bottom) showing the heterozygous peak in the parents, and a homozygous mutation in the proband. E: Structure of *GFI1B*, showing the N-terminal SNAG domain and the six C2H2 zinc finger domains

Author Manuscript Author Manuscript Author Manuscript Author Manuscript

located in the C-terminus; dashed lines indicate exon boundaries. Previously reported mutations are shown above the *GFI1B* model, while the two novel mutations described here are shown below it. F: Structural consequences of the protein-truncating mutations. Zinc fingers 4 and 5 recognize an AATC core sequence by forming base-specific hydrogen bonds between the side chains of specific amino acid residues (colored in red) and the invariant adenines and cytosine of the core sequence [28]. The side chains of residues colored in green establish hydrophobic contact with sugars or bases of DNA, while residues colored in blue establish hydrophilic electrostatic interactions with the DNA phosphodiester backbone. All contact-establishing amino acids are identical in *GFI1B* and *GFI1* in both humans and rats (the latter used for the study of DNA-GFI1B binding by nuclear magnetic resonance spectroscopy) [28].

Author Manuscript Author Manuscript Author Manuscript Author Manuscript

Table 1

Comparison of clinical, laboratory and genetic findings in families carrying *GFI1B* mutations.

	Family 1 [9,33]	Family 2 [10,11]	Family 3 [12]	Patient 1 [current paper]	Patient 2 [current paper]
Symptoms	Mild-to-severe bleeding	Easy bruising, spontaneous epistaxes, large hematomas after injuries	Mild bleeding	Petechiae; prolonged epistaxis	Spontaneous bruising; petechiae; prolonged epistaxis
Platelet count, $\times 10^9$/L (normal: 150–450)	27–80	61–129	40–115	3–67	15–50
Platelet size	Increased	Some large platelets	Variable degree of enlarged platelets	Normal MPV	Some large, hypogranular platelets
Alpha granules (normal: numerous)	Few	Some agranular platelets, some with relatively normal number	Variable degree of hypogranular platelets (LM)	Decreased	Markedly decreased
Dense bodies (mean ≥ 1.2/platelet)	N/A	Probably decreased [10] or normal [11] (only thin section EM)	N/A	0.21	0.05
Bone marrow	Dysplastic megakaryocytes, normal [33] to increased [9] in number; emperipolesis	-	-	Dysplastic megakaryocytes, decreased in number	Numerous, occasionally small megakaryocytes; emperipolesis
RBC changes	Mild anisopoikilocytosis	Anisopoikilocytosis	Abnormally shaped	Anisocytosis	-
Associated anomalies	-	-	-	PNH; hypospadias	Persistent PDA
Mutation	c.859C>T (p.Gln287*)	c.880_881insC (p.His294fs*307)	c.814+1G>C (p.G272fs*274)	c.793A>T (p.Lys265*)	c.923T>C (p.Leu308Pro)
Location	Deletion of ZF5	Disruption of ZF5	Deletion of ZF5	Disruption of ZF4 and deletion of ZF5	ZF6
Inheritance	AD (inherited)	AD (inherited)	AD (inherited)	AD (de novo)	AR

Abbreviations: AD, autosomal dominant; AR, autosomal recessive; EM, electron microscopy; LM, light microscopy; MPV, mean platelet volume; N/A, not assessed; PDA, patent ductus arteriosus; PNH, periventricular nodular heterotopia; ZF, zinc finger.